In Situ Raman Spectroscopy Investigation of the Dissociation of Methane Hydrate at Temperatures Just below the Ice Point

Takeshi Komai,* Seong-Pil Kang,† Ji-Ho Yoon,*,† Yoshitaka Yamamoto, Taro Kawamura, and Michika Ohtake

National Institute of Advanced Industrial Science and Technology, 16-1 Onogawa, Tsukuba, Ibaraki 305-8569, Japan

Received: September 24, 2003; In Final Form: March 15, 2004

Dissociation kinetics of methane hydrates was investigated by using in situ Raman spectroscopy at temperatures just below the melting point of ice. Measurements of decomposition rates were performed using finely powdered hydrate samples with a diameter range of 100−250 μm. It was found that the dissociation rate of methane hydrate at 0.1 MPa is considerably faster than that at 0.25 and 0.5 MPa. A kinetic model using non steady-state approximation and a diffusion-controlled regime is presented for describing the decomposition behavior of methane hydrates. This approach would be effective for modeling the dissociation of methane hydrate in the early stages of dissociation. The diffusion coefficients of methane molecules through the hydrate surface coated with ice are estimated to be 1.7×10^{-13}, 6.7×10^{-14}, and 2.9×10^{-14} m^2/s at 272.65, 271.15, and 268.15 K, respectively.

Introduction

Gas hydrates are non-stoichiometric inclusion compounds that are formed by the physically stable interaction between water and relatively small guest molecules occupied in the cavities built by water molecules. In general, several types of polyhedral cavity structures can be formed depending on the size and physical properties of guest molecules: structure I (sI), structure II (sII), and structure H (sH).[1,2] These structures are further arranged into well-defined three-dimensional crystalline solids.

An important practical feature of gas hydrates is that vast quantities of methane in the form of the gas hydrate exist in the permafrost zone and the subsea sediment.[3] To efficiently recover methane from gas hydrates in the deep-ocean sediments or the permafrost region, it is necessary to possess a lot of information on physicochemical properties as well as phase equilibria of gas hydrates. A large number of research articles related to gas hydrates have been published during the past 50 years, which are mainly focused on the crystalline structure and phase equilibria such as pressure−temperature behavior.

For practical applications, a thorough knowledge of decomposition behavior of gas hydrates would be of particular importance. In several works, dissociation kinetics of gas hydrates associated with depressurization or temperature ramping steps have been studied theoretically, experimentally, or morphologically.[4−14] Since there have been some unusual behaviors, such as the self-preservation effect in hydrate dissociation,[15−20] it may be difficult to clearly quantify the kinetic phenomena by observing decomposition rates with a conventional method. Thus, as shown in recent works,[4,5] in situ observation of hydrate dissociation using X-ray diffraction can be recognized as an attractive method.

The objective of this work is to investigate dissociation kinetics of methane hydrates using Raman spectroscopy. Usually, Raman spectroscopy has been used to determine the hydrate number of gas hydrates because it has advantages for accurately estimating the cage occupancy in hydrate structures.[21,22] On the other hand, Subramanian and Sloan[23] reported that the Raman spectroscopic analysis could be used for in situ observation of methane transformation to the hydrate phase from methane dissolved in water. In this contribution, we report the observation of the decomposition of methane hydrates under several dissociation conditions using Raman spectroscopy. A non-steady-state diffusion model is also examined for describing the experimentally determined dissociation kinetics.

Experimental Section

Sample Preparation. The powdered methane hydrates with an average diameter range of about 100−250 μm are used as an initial material for all experiments. The methane hydrate powder was prepared by grinding ice grains in a high-pressure cell with methane gas under the conditions of 263 K and 10 MPa for about 10 days. The reaction was monitored by carefully recording the system pressure using a pressure transducer during sample fabrication. After completion of the formation reaction, we checked for the presence of unreacted ice in the samples by X-ray diffractometry using synchrotron radiation on BL-18C at the Photon Factory, High Energy Accelerator Research Organization (KEK).[24] Thus, it was confirmed that this material consists of almost pure methane hydrate and contains a maximum of a few vol. % of ice. With measurements of weight loss on decomposition, the hydration number ($CH_4 \cdot nH_2O$) of methane hydrate samples was estimated to be 5.9 ($\pm$0.05). Small and large hydrate particles were removed with 100 and 250 μm sieves, respectively, in liquid nitrogen, and therefore we assumed that the powdered methane hydrate has a spherical shape with the diameters ranging from 100 to 250 μm. To eliminate the surface drift at a given laser spot point during dissociation runs, the methane hydrate powder is packed and shaped in pellets with a uniform size of 12 mm diameter and 6 mm thickness. Another purpose of pelletizing the hydrate samples is to give a

* Corresponding authors. E-mail: koma@ni.aist.go.jp and jihoyoon@lechem.com.

† Present address: LG Chemicals Ltd./Research Park, 104-1 Munji-dong, Yusung-ku, Taejon 305-380, Korea.

10.1021/jp0310955 CCC: $27.50
Published on Web 05/18/2004

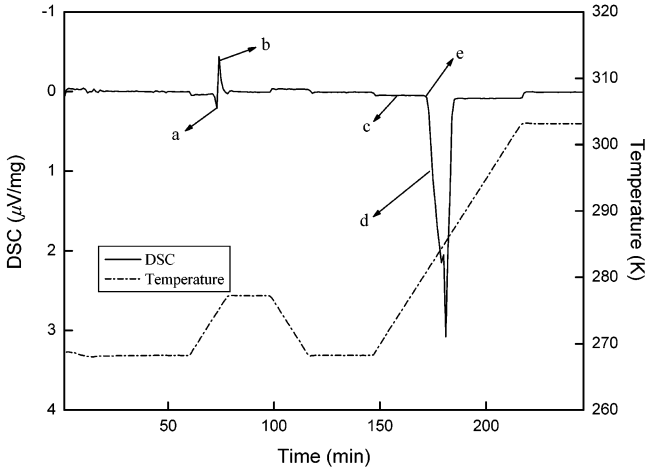

Figure 1. High-pressure DSC thermogram of methane hydrate sample at 0.5 MPa methane. (a) Peak for conversion of unreacted ice to water. (b) Peak for conversion of water (melted ice) to methane hydrate. (c) Peak for conversion of unreacted ice to water (not detected). (d) Peak for conversion of methane hydrate to water and methane gas. (e) Dissociation temperature 279.8 K (±0.2) at 0.5 MPa.

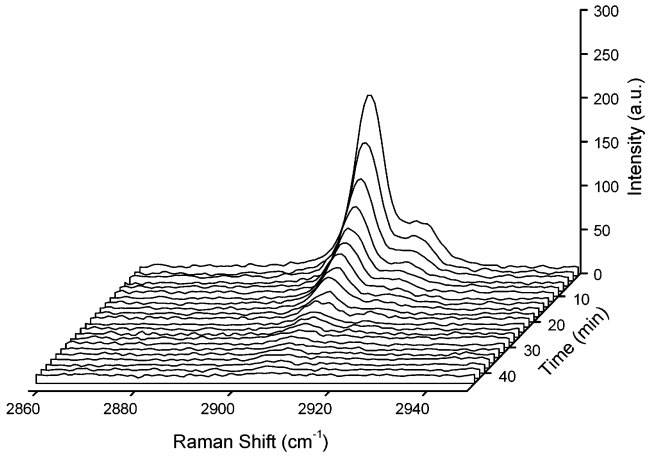

Figure 2. Time-resolved Raman spectra for the C−H stretching mode of CH_4 molecules encaged into hydrate cavities. The peaks for large and small cavities are centered at approximately 2905 and 2915 cm^{-1}. The Raman spectra were collected for about 50 min after the CH_4 hydrates were exposed under the dissociation conditions of $T = 272.65$ K and $P = 0.1$ MPa.

good heat transfer for maintaining the isothermal condition. Thus, we assume that the effect of heat of dissociation on diffusion rate of methane is negligible. The hydrate pellets with 38 ± 1% porosity were softly packed under the liquid nitrogen environment. This suggests that most of the powdered methane hydrate in the pellets may maintain its spherical form without large damages. It should be noted that, in the case of a dense packing of the ice or hydrate powder, some of the grains in a sample may be connected by bonds, and therefore the diffusion resistance of the connected layer in a mass transfer process is not negligible. However, we also note that a diffusive shrinking-core approximation might be valid only in the very beginning of the dissociation process, even in the case of the dense packing of the hydrate powder.[25]

Dissociation Procedure. A high-pressure apparatus with a temperature and pressure control system is used for in-situ observation of the decomposition rates by Raman spectrometery. The optical cell covered with a sapphire window has an internal volume of about 10 mL. Cell temperature is closely regulated by a thermo-module to within ±0.1 K, and pressure is held constant by a regulator and micrometering valve. To prevent moisture formation on the sapphire surface, dry nitrogen gas is purged continuously during the experiments. A more detailed description on the experimental apparatus is given elsewhere.[26] Initially, the cell temperature is set to about 133 K with liquid nitrogen to prevent decomposition of methane hydrates. The methane hydrate pellet is placed in the pressure cell and sealed immediately by the sapphire window. The system temperature and pressure are increased to 268 K and 5 MPa by high-pressure methane gases. For complete conversion of the remaining ice particles to methane hydrates, it is necessary to keep samples in the vessel at least for 24 h. For increasing the reaction rate, the cell temperature increases slowly (0.5 K/min) up to 278 K, and then is kept for 20∼60 min. After the reaction finished, the cell temperature is set to a desired experimental condition. Figure 1 shows a thermogram of the powdered and sieved methane hydrate at 5 MPa using a high-pressure differential scanning calorimeter (DSC). As shown in this figure, remaining ice in the samples due to incomplete conversion or decomposition during sample treatment can be completely converted into methane hydrate by a simple temperature-ramping procedure. This allows us to confirm that the amount of unreacted ice in the samples is very negligible. Prior to dissociation of methane hydrate, the system pressure is slowly decreased to the equilibrium dissociation pressure at a specified temperature, allowing the hydrate samples to reequilibrate with the gas phase at this condition. After the temperature and pressure are stabilized, the methane hydrate is dissociated by rapidly depressurizing the cell to 0.1, 0.25, or 0.5 MPa over about a 10 s interval. In this work, we do not consider the effect of rapid depressurization on variation of the system temperature, even though it may have a significant influence on the dissociation behavior. Our preliminary measurements indicate that the initial temperature differences between the sample and surroundings were about 10 K, resulting from the adiabatic temperature drop accompanying depressurization. However, the sample temperatures were completely recovered to the original surroundings within 1 min for all experimental conditions, which exhibits only minor effects of the endothermic dissociation on overall decomposition kinetics.

Raman Spectroscopy. The time-resolved measurements of hydrate dissociation using Raman spectroscopy are carried out at several pressure and temperature conditions. We use a Raman spectrometer (Jobin Yvon Ramanor T-64000) with a triple monochromator of 1800 grooves/mm grating and a CCD detector. An Ar-ion laser source emitting a 514.53 nm line is used with a power of 200 mW. The scattered radiation is collected at 180° geometry with a slit width of 250 μm, and spectra are collected with a 0.5 cm^{-1} scanning step and a 0.05 s integration time/step. Three scans are averaged to obtain each spectrum, and the signal is integrated over about 50 s for each accumulation. The calibration of the monochromator is performed regularly using the 546.09 nm line of Hg at 1122.74 cm^{-1}.

Results and Discussion

In Situ Raman Spectroscopic Observations. A typical example of the time-resolved in situ Raman spectra for dissociation of methane hydrates is shown in Figure 2. The dissociation condition, 272.65 K at 0.1 MPa, is just below the melting point of ice. It is well known that the splitting bands for methane in the hydrate indicate the partition of methane between large and small cavities in the hydrate structure I. The Raman peaks for methane molecules trapped in large $5^{12}6^4$ cages

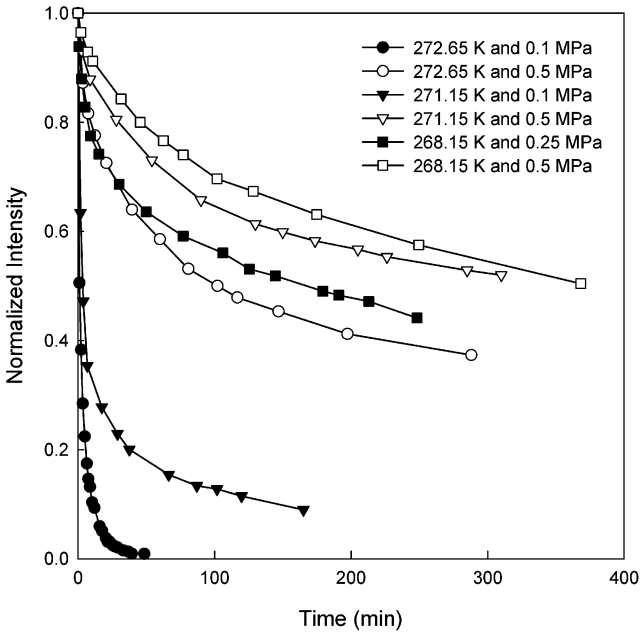

Figure 3. Integrated Raman intensity for the C−H stretching mode of CH_4 molecules encaged into large cavities as a function of time. Each peak has been normalized with respect to the intensity of Raman peak at time zero.

are centered at approximately 2905 cm^{-1}, whereas those in small 5^{12} cages are centered at approximately 2915 cm^{-1}. We note that at early times the change of Raman intensity is of significance, and therefore complete conversion of the methane hydrates to ice is finished within 1 h.

Figure 3 shows our measurement results for methane hydrate dissociation at a variety of temperature and pressure conditions. For calculation of the normalized Raman intensity, we only use the Raman peak for methane molecules in large cages because the Raman peak for methane in small cages usually overlaps with that in the gas phase at approximately 2917 cm^{-1}. At temperatures higher than 268 K, the dissociation rate of methane hydrate increases with increasing temperature,[6] whereas it decreases with increasing pressure. Further, it is noteworthy that dissociation rates of methane hydrate at 0.1 MPa are considerably faster than those at 0.25 and 0.5 MPa. This verifies that, as expected, it is essential to consider the system pressure as well as temperature for controlling dissociation rate of methane hydrates. As mentioned earlier, at 272.65 K and 0.1 MPa, we can expect complete conversion of methane hydrate to ice within 1 h. The relatively fast decomposition of methane hydrates indicates that the diffusion rate of methane molecules through the surface layer of particles coated with ice is relatively high. We also found that dissociation rates at 271.15 and 268.15 K are highly reduced after about 100 min. This may be attributed to the self-preservation effect by the surface layer coated with ice, which occurs at the dissociation of methane hydrates.[4,5,15] This also indicates that the microstructure of the surface ice or quasi-liquid layers would considerably be changed over the narrow temperature range 268−273 K, in which the formation of ice layer occurs under a condition of relatively low pressure (no higher than 1.0 MPa). Thus, for more accurate understanding of the self-preservation effect, a detailed observation of the microstructure of the surface layer such as microfractures attending the volume change between the hydrate and ice, as well as physical properties typified by strength and permeability of surface layer, should be in progress.

Kinetic Model for Hydrate Dissociation. As indicated previously, we have used the finely powdered methane hydrates with diameters ranging from 100 to 250 μm. We also assume that the hydrate dissociation is governed by a diffusion-controlled dissociation step. Therefore, the starting point for the description of dissociation of methane hydrates is the non-steady-state approximation to molecular diffusion of methane in a sphere. The governing equation comes from Fick's law of diffusion as follows:

$$\frac{\partial C}{\partial t} = D\frac{1}{r^2}\frac{\partial}{\partial r}\left(r^2\frac{\partial C}{\partial r}\right) \tag{1}$$

where C is the concentration of methane in the hydrate particles, r is the radius of the hydrate particles, and D is the diffusion coefficient of methane in the ice layer. If we consider the flux of methane through the spherical wall of the ice layer, the initial and boundary conditions are given by

$$\begin{aligned} C &= C_B \quad t = 0 \\ C &= C_B \quad t > 0 \quad r = r_0 \\ C &= C_H \quad t > 0 \quad r = x(t) \end{aligned} \tag{2}$$

Here, C_H and C_B are the concentration of methane in hydrate and bulk gas phases, respectively, r_0 is the initial hydrate radius, and $x(t)$ is the radius of hydrate depending on the elapsed time. Hence, using these initial and boundary conditions, the general solution of the diffusion equation can be obtained as a function of the hydrate radius and elapsed time:[27,28]

$$\tilde{C} = \frac{C - C_B}{C_H - C_B} = \frac{x(r_0 - r)}{r(r_0 - x)} - \frac{2x}{\pi r}\sum_{n=1}^{\infty}\frac{1}{n}\sin\frac{n\pi(r - x)}{r_0 - x}\exp\left(-\frac{n^2\pi^2 Dt}{(r_0 - x)^2}\right) \tag{3}$$

This equation represents the concentration profile of methane in the ice layer between r_0 and $x(t)$. To our knowledge, there is no significant gradient in the concentration of methane at the interface between the hydrate particle and the bulk gas phase, $r = r_0$. In contrast, it should be noted that the concentration gradient at the moving boundary $r = x(t)$ is related to the rate of dissociation, that is, the rate of interface movement. Hence we may write

$$\frac{dx(t)}{dt} = \phi D\frac{\partial \tilde{C}}{\partial r}\Big|_{r=x(t)} \tag{4}$$

For hydrate dissociation, a dimensionless parameter ϕ should be a constant of proportionality characteristic of the system at the dissociation condition. To give the driving force for hydrate dissociation, we see that

$$\phi = \frac{f_{EQ} - f_B}{f_B - f^*} \tag{5}$$

where f_{EQ} stands for the equilibrium fugacity of methane in the gas phase at the dissociation pressure of methane hydrate at temperature T, and f_B is the fugacity of methane in the gas phase at the decomposition condition, which are calculated by our model developed in previous work.[29] The above representation is based on the fact that the decomposition rate of methane hydrate will be proportional to $P_{EQ}(1/P_B - 1/P_{EQ})$ at a given

temperature T.[11,30] We note that the correction parameter $f^* = f^*(T)$ can be obtained as a function of temperature to give a diffusion coefficient for different pressure conditions. As previously mentioned, when the granular samples of the methane hydrate are exposed to the decomposition condition at which the methane hydrate could be unstable, the diffusion rates of methane through the surface layer of ice depend not only on the decomposition condition but also on microstructure of the surface layer. In our considerations, the correction parameter is required for compensating a small difference of the diffusion coefficients obtained at a given temperature, but at different pressures at which the ice surface layer may practically have different morphology. Hence, it likely allows us to obtain the diffusion coefficient of methane through the surface ice layer regardless of the dissociation pressures.

For the initial period of hydrate dissociation $x \cong r_0$ and $t \cong 0$, it is possible to assume that a similarity parameter $\xi = (r_0 - x)/\sqrt{Dt}$ is nearly constant. Based on this approximation, solving eqs 3 and 4 simultaneously gives

$$\frac{1}{2}\xi^2 = \phi\left[\frac{r_0}{x} + 2\sum_{n=1}^{\infty}\exp\left(-\frac{n^2\pi^2}{\xi^2}\right)\right] \cong \phi\left[1 + 2\sum_{n=1}^{\infty}\exp\left(-\frac{n^2\pi^2}{\xi^2}\right)\right] \quad (6)$$

As expected, it is likely that, for a small time interval, the value of ξ can be determined to be a constant and depends on the parameter ϕ, that is, the dissociation condition T and P. Using the determined value ξ, the relationship between the integrated Raman intensity $I(t) \cong [x(t)/r_0]^3$and the elapsed time t is given by

$$\frac{(1 - I(t)^{1/3})^2}{\xi^2} = \frac{Dt}{r_0^2} \quad (7)$$

As stated previously, we assume that the non-steady-state approximation plays a key role in describing decomposition of methane hydrate, resulting from diffusion of methane through the ice layer. In this work, we take into account only the initial dissociation rates to minimize a shielding or crack effect of the ice layer during dissociation, resulting in diffusion of methane through micropores and crack boundaries. As pointed out by previous workers,[4,5] the high diffusion coefficient of methane in dissociation experiments is caused by enhancement of decomposition rates dominated by the diffusion of methane through these micropores and crack boundaries. A sharp decrease in dissociation rates at earlier times is observed for all dissociation conditions, as can be seen in Figure 3. Figures 4 and 5 show plots of dissociation results in terms of eq 7 for each temperature and pressure condition.

A linear relationship by plotting $(1 - I(t)^{1/3})^2/\xi^2$ as a function of t must hold at earlier times, as shown in Figure 5. This indicates that our experimental data agree with the non-steady-state approximation and diffusion-controlled dissociation regime. Of particular interest is, however, that the decomposition rates at 272.65 K follow the linear relationship even until approximately 85% conversion of methane hydrates. When assuming an average size of hydrate particles of 175 μm, 85% conversion corresponds to an ice layer with a thickness of 50 μm. To clarify the kinetics of dissociation of methane hydrates, it may be necessary to take into account additional factors such as the heat transfer effect and temperature lowering by heat of dissociation or Knudsen diffusion through micropores.

Diffusion Coefficients. The diffusion coefficient depends on the temperature and the initial grain size of the methane hydrate. This is consistent with our experimental results observed at different temperature and pressure conditions as shown in Figures 4 and 5. Using the slopes in Figure 5 and eq 7, the diffusion coefficients of methane through the ice layer are calculated to be 1.7×10^{-13}, 6.7×10^{-14}, and 2.9×10^{-14} at 272.65, 271.15, and 268.15 K, respectively. An abrupt increase of the diffusion coefficient with a small increase of temperature is observed for this temperature range. It is likely that the temperature dependence of the diffusion coefficients does not follow Arrhenius behavior. It should be emphasized that, as indicated by previous researchers,[6,11,16] there has been no definitive conclusion for dissociation kinetics of gas hydrates. In particular, the temperature range studied in this work is just below the melting point of ice. Thus, as previously mentioned, unusual dissociation behavior over the narrow thermal range 268−273 K may be caused by a significant change of microstructure of the surface layer due to the volume change and possible stresses imposed at the granular scale. In comparison, the calculated dissociation coefficients are 2 orders of magnitude lower than the values estimated from a shrinking core model by previous workers.[4,5] This discrepancy might also be attributed to different experimental conditions, different sample treatment such as annealing of the samples, different pressure−temperature processing, inadequate assumption, or long-reaction time scale, indicating that the methane molecules dominantly diffuse out through fine pores and crack boundaries. For instance, when we assume the steady-state approximation,[4,5] solving eqs 3 and 4 simultaneously gives

$$3(1 - I(t)^{2/3}) - 2(1 - I(t)) = \phi\frac{6Dt}{r_0^2} \quad (8)$$

The resulting equation is very similar to that derived by previous workers[4,5] except for the characteristic constant ϕ. If the steady-state approximation about diffusion is valid, a plot of $3(1 - I(t)^{2/3}) - 2(1 - I(t))$ vs t should be a straight line over a whole time scale. As shown in Figure 6, the dissociation behavior at earlier times is not on the straight line fit to the later times. It is likely that the dissociation data only after about 100 min give straight lines, indicating the steady-state diffusion. Thus, the dissociation behavior of methane hydrate at the beginning, especially at temperatures just below the ice point, does not follow the steady-state diffusion approximation. Another possible explanation is that the decomposition rates of gas hydrates depend strongly on the sample conditions . For instance, if we use the hydrate particles coated with fine ice crystals, it may be impossible to expect the same result. However, we believe that our results presented in this article may provide a basic knowledge for understanding the dissociation behavior of gas hydrates at temperatures just below the meting point of ice. Very recently, the diffusion coefficient of methane in hexagonal ice has been estimated by a theoretical model based on the molecular orbital method.[31] Of particular interest is that the estimated value was found to be 2.0×10^{-14} m^2/s, which is the same order of magnitude as our experimental values.

In this study, we assume that the dissociation rate of methane hydrate is controlled by the diffusion of methane molecules through the layers of ice covering the hydrate particles. The rate-limiting step at the starting point should be the breaking of the hydrogen bonds in the hydrate structure. However, once a thin layer of ice is produced by partial decomposition of the hydrate surface, the process would be controlled by the diffusion rate of methane molecules through the accumulating ice layers.

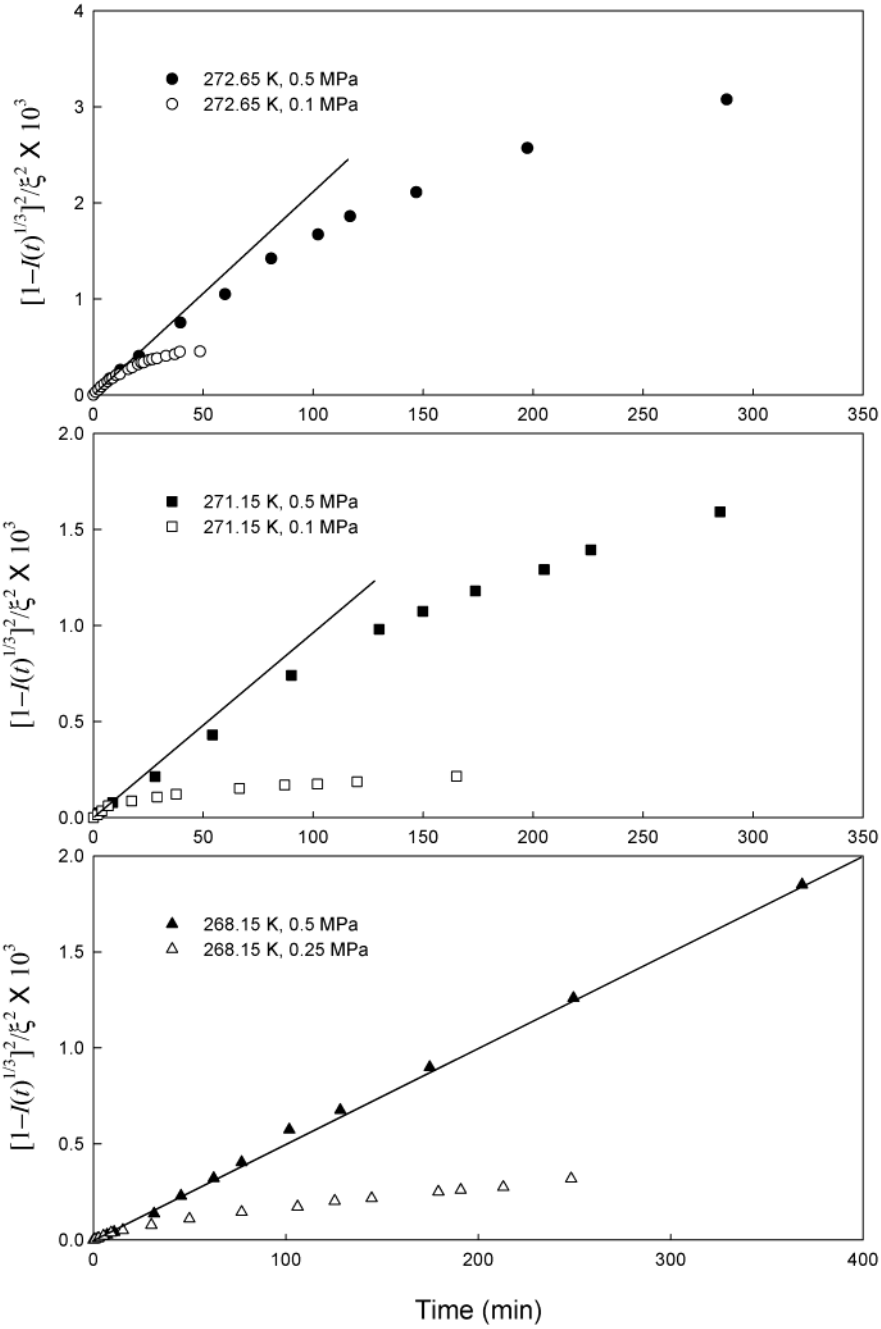

Figure 4. Plot of experimental data for dissociation of methane hydrates in terms of a non-steady-state diffusion model based on eq 7. As a starting material, finely powdered methane hydrates with diameters ranging from 100 to 250 μm are taken into account for the model. The parameter ξ depending on the dissociation condition T and P is calculated using eq 6.

Similarly, this two-stage dissociation has been observed by Davison et al.[32] for the dissociation of krypton hydrate and Takeya et al.[4,5] for methane hydrate at low temperatures. Figure 7 shows high-pressure DSC thermograms for dissociation of the methane hydrate near each equilibrium temperature at three different pressures. It is clear that a strong shielding effect of the ice layers occurs at low pressures below 1 MPa. This may be attributed to an elevated internal methane pressure in the hydrate core. As mentioned earlier, the diffusion coefficient of dissociated methane in hexagonal ice should be one of the most important factors to control the internal pressure. It has been proposed that the transport of gas molecules to the outer surface in granular samples might be inhibited because a higher pressure could be maintained in the interior of the sample, which allows the establishment of a local region of near equilibrium in the interior.[33] Our measurements and calculations[29] indicate that the increase of the internal pressure in the hydrate core by the surface layer initially coated with ice is less than 0.05 MPa over the temperature range 213−273 K. We note that the effect of the elevated internal pressure on the hydrate dissociation at high pressures is very negligible, and therefore the difference between the equilibrium temperature and dissociation temperature measured by using DSC at 1.6 MPa is less than 0.4 K. At this dissociation condition, the maximum increase of the internal pressure is expected to be 0.03 MPa. In contrast, the dissociation temperature measured by DSC at 0.2 MPa is found to be 213.1 K ($\pm$0.2 K) as shown in Figure 7 (the first peak). This temperature is 4.7 K higher than the equilibrium temperature, even though the maximum increase of the internal pressure would be 0.05 MPa. These experimental measurements were

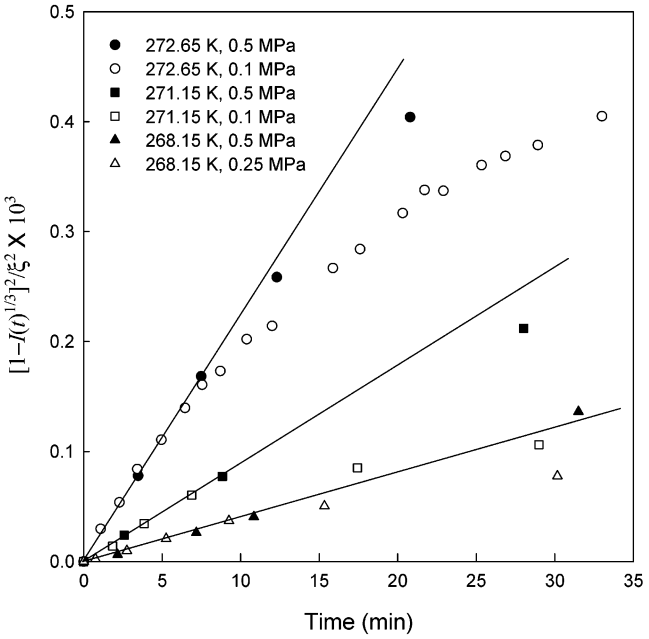

Figure 5. Plot of experimental data for dissociation of methane hydrates at near initial dissociation. The diffusion coefficients of methane through the ice layer are calculated using the slope of initial dissociation rates.

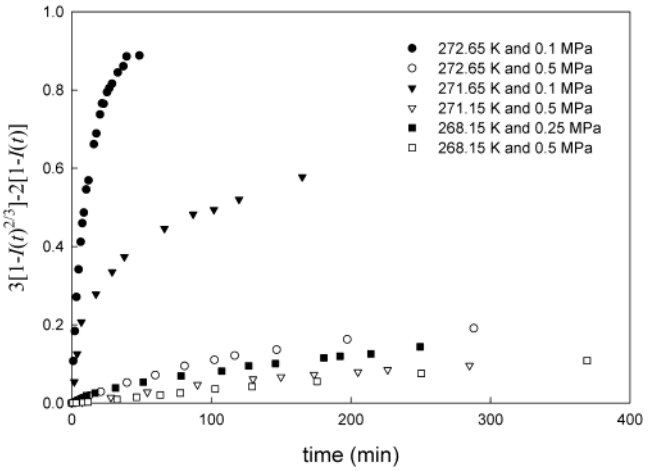

Figure 6. Plot of experimental data for dissociation of methane hydrates in terms of steady-state diffusion model based on eq 8.

quite reproducible when we used the same hydrate sample. It should be noted, however, that the annealing condition and granular size of the methane hydrate have profound effects on the elevated internal pressure by the surface layer of ice during the dissociation runs. When the experiments with DSC were performed at the same pressures but with different annealing conditions and the methane hydrate having different granular size, the dissociation temperature was largely shifted from the equilibrium temperature at a given pressure. These findings support the diffusion-controlled dissociation of methane hydrate basically assumed in this work.

Summary

We provide here the experimental and theoretical results for conversion of methane hydrates to ice observed using in situ Raman spectroscopy at temperatures just below the melting point of ice. As a starting material, finely powdered methane hydrates with diameters ranging from 100 to 250 μm are used for these experiments. It was found that the dissociation rate of methane

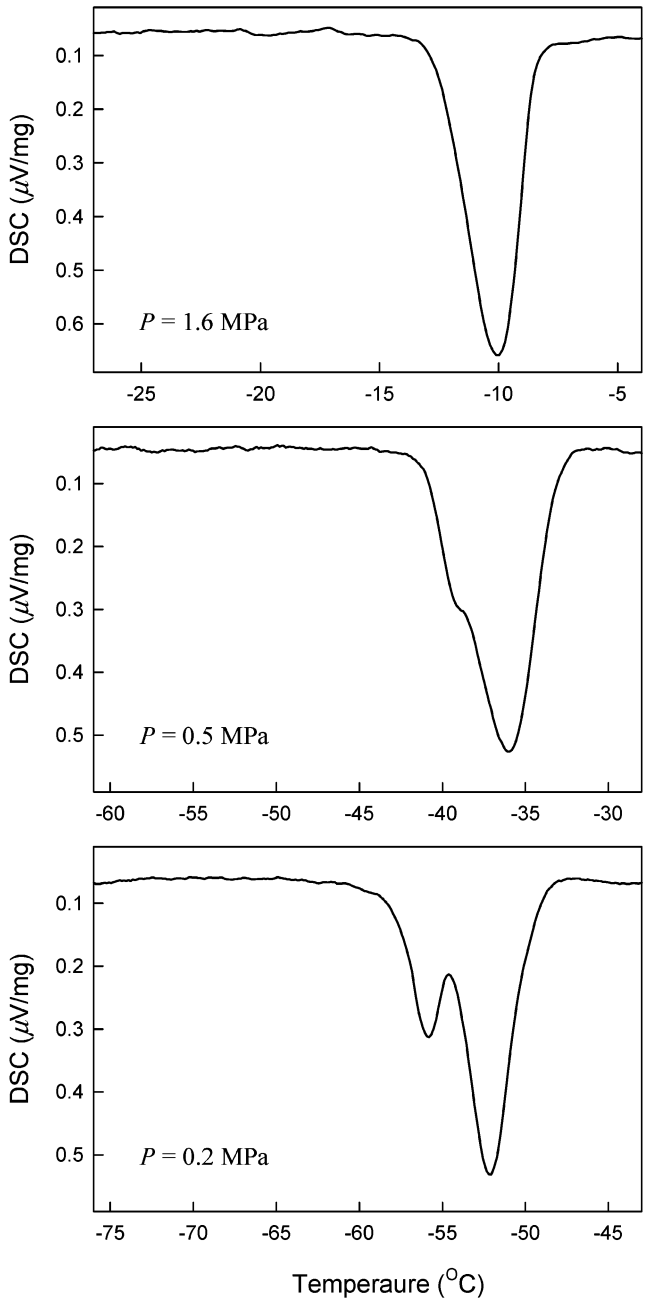

Figure 7. High-pressure DSC thermogram of methane hydrate sample at 0.2, 0.5, and 1.6 MPa methane. The temperature increasing rate is 0.5 K/min for all runs.

hydrates increases with increasing temperature, whereas it decreases with increasing pressure. A relatively fast decomposition of methane hydrates at 272.65 K and 0.1 MPa was observed, indicating that the diffusion rate of methane molecules through hydrate particles coated by the ice layers is relatively high. Based on the non-steady-state approximation, the dissociation behavior of methane hydrate was described in terms of the diffusion-controlled reaction regime. The diffusion coefficients of methane molecules through the ice layer were calculated by fitting the model to experimental data. Recently, it has been proposed that the maximum possible rate at which the dissociation can take place would be achieved only if the experiments are carried out such that the pressure of the gas has no effect on the decomposition rate (i.e., under vacuum).[11,12] One may argue that there is some of difficulty in the decomposition measurements in a vacuum, such as a rapid evaporation of the surface

layer of ice, resulting in the change of microstructure or further fracture of the surface layer. It is clear, however, that the measurements of the limiting decomposition rate in a vacuum become of primary interest in studying the decomposition kinetics of the methane hydrate; thus it may be a powerful way for a broad understanding of the diffusion process of methane molecules through the surface layer of ice.

Acknowledgment. We thank Drs. Y. Sakamoto and Y. Kawabe for their valuable comments on the kinetic model. This work was supported in part by the JSPS fellowship program of Japan Society for the Promotion of Science.

References and Notes

(1) Sloan, E. D., Jr. *Clathrate Hydrates of Natural Gases*, 2nd ed.; Marcel Dekker: New York, 1998.
(2) Ripmeester, J. A.; Tse, J. S.; Ratcliffe, C. I.; Powell, B. M. *Nature* **1987**, *325*, 135.
(3) Kvenvolden, K. A. *Proc. Natl. Acad. Sci. U.S.A.* **1999**, *96*, 3420.
(4) Takeya, S.; Shimada, W.; Kamata, Y.; Ebinuma, T.; Uchida, T.; Nagao, J.; Narita, H. *J. Phys. Chem. A* **2001**, *105*, 9756.
(5) Takeya, S.; Ebinuma, T.; Uchida, T.; Nagao, J.; Narita, H. *J. Cryst. Growth* **2002**, *237*−*239*, 379.
(6) Stern, L. A.; Circone, S.; Kirby, S. H.; Durham, W. B. *J. Phys. Chem. B* **2001**, *105*, 1756.
(7) Stern, L. A.; Circone, S.; Kirby, S. H.; Durham, W. B. *Energy Fuels* **2001**, *15*, 499.
(8) Kelkar, S. K.; Selim, M. S.; Sloan, E. D. *Fluid Phase Equilib.* **1998**, *150*−*151*, 371.
(9) Servio, P.; Englezos, P. *AIChE J.* **2003**, *49*, 269.
(10) Ji, C.; Ahmadi, G.; Smith, D. H. *Chem. Eng. Sci.* **2001**, *56*, 5801.
(11) Wilder, J. W.; Smith, D. H. *J. Phys. Chem. B* **2002**, *106*, 6298.
(12) Wilder, J. W.; Smith, D. H. *J. Phys. Chem. B* **2002**, *106*, 226.
(13) Stern, L. A.; Circone, S.; Kirby, S. H.; Durham, W. B. *J. Phys. Chem. B* **2002**, *106*, 228.
(14) Uchida, T.; Ebinuma, T.; Narita, H. *J. Cryst. Growth* **2000**, *217*, 189.
(15) Yakushev, V. S.; Istomin, V. A. *Physics and Chemistry of Ice*; Hokkaido University Press: Sapporo, 1992.
(16) Stern, L. A.; Kirby, S. H.; Durham, W. B. *Science* **1996**, *273*, 1843.
(17) Stern, L. A.; Kirby, S. H.; Durham, W. B. *Energy Fuels* **1998**, *12*, 201.
(18) Stern, L. A.; Hogenboom, D. L.; Durham, W. B.; Kirby, S. H.; Chou, I.-M. *J. Phys. Chem. B* **1998**, *102*, 2627.
(19) Moudrakovski, I. L.; Ratcliffe, C. I.; McLaurin, G. E.; Simard, B.; Ripmeester, J. A. *J. Phys. Chem. A* **1999**, *103*, 4969.
(20) Stern, L. A.; Kirby, S. H.; Durham, W. B. *J. Phys. Chem. A* **2001**, *105*, 1223.
(21) Sum, A. K.; Burruss, R. C.; Sloan, E. D., Jr. *J. Phys. Chem. B* **1997**, *101*, 7371.
(22) Uchida, T.; Hirano, T.; Ebinuma, T.; Narita, H.; Gohara, K.; Mae, S.; Matsumoto, R. *AIChE J.* **1999**, *45*, 2641.
(23) Subramanian, S.; Sloan, E. D., Jr. *Fluid Phase Equilib.* **1999**, *158*−*160*, 813.
(24) Hirai, H.; Uchihara, Y.; Fujihisa, H.; Sakashita, M.; Katoh, E.; Aoki, K.; Nagashima, K.; Yamamoto, Y.; Yagi, T. *J. Chem. Phys.* **2001**, *115*, 7066.
(25) Staykova, D. K.; Kuhs, W. F.; Salamatin, A. N.; Hansen, T. *J. Phys. Chem. B* **2003**, *107*, 10299.
(26) Kawamura, T.; Takeshi, T.; Yamamoto, Y.; Nagashima, K.; Ohga, K.; Higuchi, K. *J. Cryst. Growth* **2002**, *234*, 220.
(27) Carslaw, H. S.; Jaeger, J. C. *Conduction of Heat in Solids*, 2nd ed.; Oxford University Press: Oxford, 1946.
(28) Crank, J. *The Mathematics of Diffusion*, 2nd ed.; Oxford University Press: Oxford, 1975.
(29) Yoon, J.-H.; Chun, M.-K.; Lee, H. *AIChE J.* **2002**, *48*, 1317.
(30) Searcy, A. W.; Beruto, D. *J. Phys. Chem.* **1978**, *82*, 163.
(31) Hori, A.; Hondoh, T. *Can. J. Phys.* **2003**, *81*, 251.
(32) Davison, D.; Garg, S.; Gough, S.; Handa, Y.; Ratcliffe, C.; Ripmeester, J.; Tse, J. *Geochim. Cosmochim. Acta* **1986**, *50*, 619.
(33) Beruto, D.; Searcy, A. W. *J. Chem. Soc., Faraday Trans.* **1974**, *70*, 2145.